

Operational Properties of Ridge Waveguide Lasers with Laterally Tapered Waveguides for Monolithic Integration

Oh Kee Kwon, Ki Soo Kim, Jae Sik Sim, and Yong Soon Baek

ABSTRACT—We report on a ridge waveguide laser diode with laterally tapered waveguides fabricated in a single growing step using a double patterning method. In this structure, nearly constant output power is obtained with the change of the lower tapered waveguide width, and the facet power ratio of 1.4 to 1.5 is observed over the current range. The asymmetric facet power property is also investigated.

Keywords—Monolithic integration, optical waveguide, optical coupling, asymmetric facet power, internal reflection.

I. Introduction

In order to fabricate a monolithically integrated device, such as a tunable laser [1], [2], a multi-wavelength laser [3], or a wavelength converter [4], several waveguide structures for each functional section should be smoothly connected to each section of the device. A number of waveguide coupling structures have been developed to allow for materials optimization suitable for each separate photonic function [5]. In particular, an evanescent-coupling structure enables a simple fabrication process requiring only partial etching of the active region in the passive section without any re-growth process. However, in order to obtain stable optical power transfer, the tip width should be less than 1 μm [5], [6], which is usually very difficult to realize with conventional photolithography and dry etching. In this letter, we present a

ridge waveguide laser diode (RWG LD) with tapered waveguides. It is easily fabricated by using lithography with two different masks by turns. We also investigate its operational properties experimentally.

II. Device Structure and Fabrication

Figure 1 shows a schematic view of the device, which is composed of a shallow ridge (SR) section with a ridge width of $w_s=2.8 \mu\text{m}$ and a deep ridge (DR) section with two tapered waveguides. The upper two-step tapered waveguide structure was designed to smoothly transfer the optical mode generated by the active layer into a passive guide ($w_{t1}=2 \mu\text{m}$, $w_{t2}=4.3 \mu\text{m}$, $L_{t1}=180 \mu\text{m}$, $L_{t2}=50 \mu\text{m}$, $L_b=50 \mu\text{m}$), and the lower tapered waveguide was selected to examine the mode-size conversion and the power transfer property with respect to w_d (3 to 4.5 μm). The active region contains a multiple quantum well (MQW) and a two-step separate confinement hetero-structure (SCH) layer. The passive guide consists of 0.195, 0.18, and 0.165 μm InGaAsP layers with 1.24 μm bandgap wavelength interleaved between 0.45 μm thick InP layers [5].

For the fabrication of the upper waveguide structure, the tapered waveguide mask pattern was formed by using photolithography and silicon-nitride dry etching (magnetically enhanced reactive ion etching) with two different masks (masks 1 and 2) in sequence. Then, the 7°-tilted SR section mask pattern (photo-resist, PR) was made by photolithography. The dry etching (reactive ion etching) was performed to a depth of approximately 1.2 μm (the thickness of the upper cladding layer=1.8 μm). After the removal of the PR mask from the SR section, additional dry etching was done near the lower SCH

Manuscript received July 18, 2007; revised Sept. 28, 2007.

This work was supported by the IT R&D program of MIC/IITA, Rep. of Korea [2007-S001-01, Development of Optical Switches for ROADM].

Oh Kee Kwon (phone: + 82 42 860 1366, email: okkwon@etri.re.kr), Ki Soo Kim (email: kimks1136@etri.re.kr), Jae Sik Sim (email: jssim@etri.re.kr), and Yong Soon Baek (email: yongb@etri.re.kr) are with the IT Convergence & Components Laboratory, ETRI, Daejeon, Rep. of Korea.

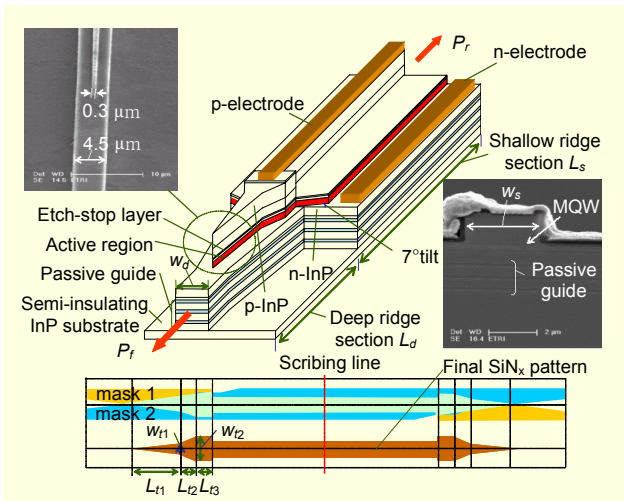


Fig. 1. Schematic diagram of the RWG LD with laterally tapered waveguides.

InGaAsP layer. Micro-ashing and H_2SO_4 treatment were added to remove residual polymers attached to the etched walls. The shallow ridge shape in the SR section was formed to the etch-stop layer using selective InP wet etching after the opening of the pattern slightly longer than the SR section with PR mask. In this case, the outside of the SR section within the opening pattern is not attacked due to the InGaAsP layer. The InGaAsP wet etching was performed after the removal of the PR mask. A tip width of about $0.3 \mu\text{m}$ was achieved.

III. Results and Discussion

Figure 2 shows the output power-versus-current (P - I) characteristics of a $600 \mu\text{m}$ long solitary RWG LD and those of integrated LDs with $w_d=3, 3.5, 4, 4.5 \mu\text{m}$, $L_s=600 \mu\text{m}$, and $L_d=400 \mu\text{m}$ under CW operation at 22°C . Output powers are gradually saturated with current I because of the relatively high series resistance R_s ($\approx 6.8 \Omega$) which can result from current crowding in the n-InP layer between the active region and passive guide. By introduction of the tapered waveguides, the front-facet slope efficiency of the integrated LD is increased, and the output power is higher than that of the solitary LD at $I > 160 \text{ mA}$, despite the increase of the threshold current. This is mainly due to the optical absorption of the active region in the DR section. Obviously, the output powers remain nearly constant with the change of w_d . This means that the mode size can be converted without the additional losses caused by w_d . The output power at the front (tapered) facet P_f differs from that at rear P_r in slope efficiency as in [7] and [8]. The facet power ratio P_f/P_r of 1.4 to 1.5 is obtained over the current range. It is difficult to clearly explain this phenomenon in the integrated LD because, in the composite cavity, the passive

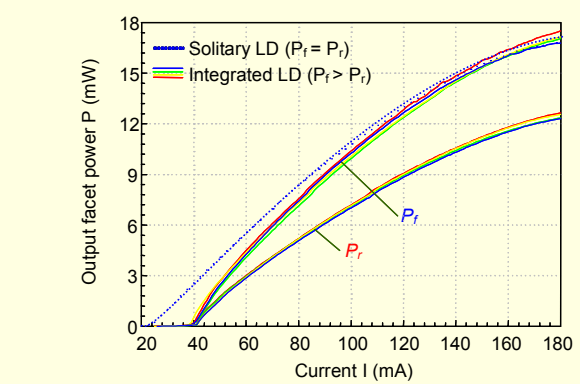


Fig. 2. P - I characteristics of a $600 \mu\text{m}$ long solitary LD (dotted line) and integrated LDs with $w_d=3, 3.5, 4, 4.5 \mu\text{m}$, $L_s=600 \mu\text{m}$, and $L_d=400 \mu\text{m}$ (solid lines) under CW operation (22°C).

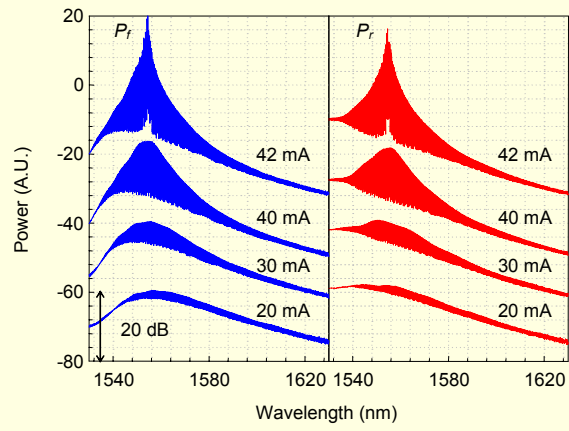


Fig. 3. ASE spectra at the front facet (left) and the rear (right) for the integrated LD ($w_d=3.5 \mu\text{m}$) at currents of 20, 30, 40, and 42 mA.

section optical loss and longitudinal spatial hole burning (LSHB) cause the asymmetry of intensity distribution only within the gain section. Besides, the converted mode size has hardly any influence on the facet reflectivity. Figure 3 shows amplified spontaneous emission (ASE) spectra at the front (left) and rear facet (right) for the integrated LD ($w_d=3.5 \mu\text{m}$) at currents of 20, 30, 40, and 42 mA, respectively. Compared to the spectral powers at the rear facet, those at the front are relatively reduced near $1,540 \text{ nm}$ due to the absorption loss in the DR section. However, as a result of faster peak increase with the current, they show higher powers near the threshold. On the other hand, it was found that the lasing peak wavelength of the integrated LD (about $1,554 \text{ nm}$) was longer than that of the solitary LD (about $1,547 \text{ nm}$) in spite of the increase of the threshold current (band-filling effect). This is because absorption becomes dominant for the photons with higher energy (shorter wavelength), which makes the gain

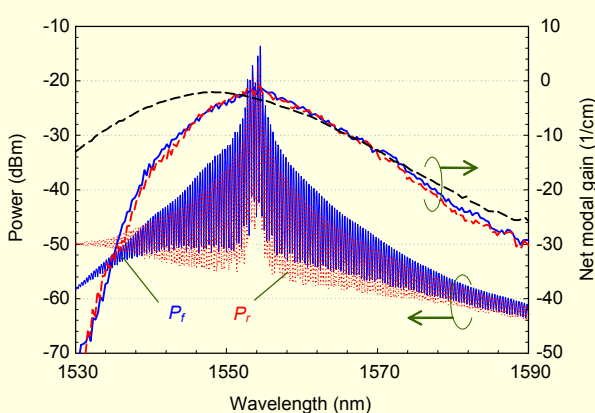


Fig. 4. ASE spectra of the integrated LD at front (P_f , solid blue line) and the rear (P_r , dotted red line), and net modal gains of solitary LD (black dashed line) and integrated LD.

spectral width narrow and the gain peak shift to a longer wavelength. Figure 4 shows the ASE spectra of the integrated LD at $I=44$ mA and the net modal gains of the solitary LD and the integrated LD. The gain peak wavelengths of the integrated LD are at longer wavelengths than those of solitary LD as expected. It is clearly shown that the spontaneous emission of the front facet is higher than that of the rear within the wavelength range from 1,539 to 1,580 nm, while both modal gains are nearly the same. For this result, we think the increase of the spontaneous emission results in higher slope efficiency via the increase of internal quantum efficiency.

IV. Conclusion

We fabricated RWG LDs with tapered waveguides (with a tip width of about $0.3\text{ }\mu\text{m}$) by using a double patterning method and investigated their operational properties. The fabricated device showed stable operation and its performance was uniform because it has no re-growing process. The output powers of integrated LDs remained nearly constant with the change of w_d . The facet power ratio P_f/P_r of 1.4 to 1.5 was obtained over the current range. It was also found that this asymmetry of the facet power results from the wavelength dependency of active layer absorption in the DR section, which makes the spontaneous emission of the front facet increase near the gain peak. We think this structure is suitable for monolithic integration of various devices without requiring epitaxial re-growth.

References

- [1] O.K. Kwon, E.D. Sim, K.H. Kim, J.H. Kim, H.G. Yun, O.K. Kwon, and K.R. Oh, "Widely Tunable Grating Cavity Laser," *ETRI Journal*, vol. 28, no. 5, 2006, pp. 545-554.

- [2] S.H. Oh, H. Ko, K.S. Kim, J.M. Lee, C.W. Lee, O.K. Kwon, S. Park, and M.H. Park, "Fabrication of Butt-Coupled SGDBR Laser Integrated with Semiconductor Optical Amplifier Having a Lateral Tapered Waveguide," *ETRI Journal*, vol. 27, no. 5, 2005, pp. 551-556.
- [3] O.K. Kwon, K.H. Kim, E.D. Sim, J.H. Kim, and K.R. Oh, "Monolithically Integrated Multiwavelength Grating Cavity Laser," *IEEE Photon. Technol. Lett.*, vol. 17, no. 9, 2005, pp. 1788-1790.
- [4] H.S. Kim, J.H. Kim, E.D. Sim, Y.S. Baek, K.H. Kim, O.K. Kwon, and K.R. Oh, "All-Optical Mach-Zehnder Interferometric Wavelength Converter Monolithically Integrated with Loss-Coupled Distributed Feedback Probe Source," *Japanese Journal of Applied Physics*, vol. 42, no. 7B, July 2003, pp. L831-L833.
- [5] V.M. Menon, F. Xia, and S.R. Forrest, "Photonic Integration Using Asymmetric Twin-Waveguide (ATG) Technology: Part II-Device," *IEEE J. Select. Topics in Quantum Electron.*, vol. 11, no. 1, 2005, pp. 30-42.
- [6] H. Bissessur, C. Graver, O.Le. Gouezigou, G. Michaud, and F. Gaborit, "Ridge Laser with Spot-Size Converter in a Single Epitaxial Step for High Coupling Efficiency to Single-Mode Fiber," *IEEE Photon. Technol. Lett.*, vol. 10, no. 9, 1998, pp. 1235-1237.
- [7] A. Lestra and J.-Y. Emery, "Monolithic Integration of Spot-Size Converters with $1.3\text{-}\mu\text{m}$ Lasers and $1.55\text{-}\mu\text{m}$ Polarization Insensitive Semiconductor Optical Amplifiers," *IEEE J. Select. Topics Quantum Electron.*, vol. 3, Dec. 1997, pp. 1429-1440.
- [8] S.W. Ryu, S.B. Kim, J.S. Sim, J. Kim, "1.55- μm Spot-Size Converter Integrated Laser Diode with Conventional Buried-Heterostructure Laser Process," *IEEE Photon. Technol. Lett.*, vol. 15, no. 1, 2003, pp. 12-14.